Available online at www.sciencedirect.com
ScienceDirect
Trans. Nonferrous Met. Soc. China 31(2021) 2013−2023
Transactions of Nonferrous Metals Society of China
www.tnmsc.cn

Impact of replacement of Re by W on dislocation slip mediated creeps of γ'-Ni_3Al phases

Zhou YI, Yun-lei XU, Ping PENG, Jiang-hua CHEN

School of Materials Science and Engineering, Hunan University, Changsha 410082, China

Received 6 August 2020; accepted 18 February 2021

Abstract: The anomalous flow behavior of γ'-Ni_3Al phases at high temperature is closely related to the cross-slip of 1/2⟨110⟩{111} super-partial dislocations. Generalized stacking fault energy curves (i.e., Γ-surfaces) along the lowest energy path can provide a great deal of information on the nucleation and movement of dislocations. With the first-principles calculation, the interplay between Re and W, Mo, Ta, Ti doped at preferential sites and their synergetic influence on Γ-surfaces and ideal shear strength (τ_{max}) in γ'-Ni_3Al phases are investigated. Similar to single Re-addition, the Suzuki segregation of W at stacking faults is demonstrated to enable to impede the movement of 1/6⟨112⟩{111} Shockley partial dislocations and promote the cross-slip of 1/2⟨110⟩{111} super-partial dislocations. With the replacement of a part of Re by W, a decreased $\gamma_{APB}^{111}/\gamma_{APB}^{001}$ indicates that the anomalous flow behavior of γ' phases at high temperature is not as excellent as the double Re-addition, but an increased τ_{max} means that the creep rupture strength of Ni-based single crystal superalloys can be benefited from this replacement to some extent, especially in the co-segregation of Re and W at Al−Al sites. As the interaction between $X1_{Al}$ and $X2_{Al}$ point defects is characterized by an correlation energy function $\Delta E^{X1_{Al}+X2_{Al}}(d)$, it is found that both strong attraction and strong repulsion are unfavarable for the improvement of yield strengths of γ' phase.

Key words: Ni-based single crystal superalloy; γ'-Ni_3Al; generalized stacking fault energy; ideal shear strength; dislocation; cross-slip

1 Introduction

Ni-based single crystal (SC) superalloys are widely applied in most aero-engine combustors, because of outstanding ability to retain strength and withstand creep at high temperature [1,2]. Their excellent comprehensive performances rely primarily on the microstructure of γ' precipitates with $L1_2$ structure embedded coherently in fcc γ matrixes [3], as well as many kinds of refractory elements such as Re, W, Mo, Ta, Ti, Cr, and Ru. Re is proven to be a crucial element in the creep of Ni-based SC superalloys, and the indispensable strengthening is usually called as Re-effect [4]. However, an excessive addition of Re leads to some detrimental topologically close-packed (TCP) phases to be deposited [5]. Also, a limited reserve of this expensive Re element motivates the development of low Re-addition superalloys. Recently, several investigations [6,7] have demonstrated that Re can be partially replaced by other refractory metals. For example, as a half amount of Re in CMSX-4 superalloys is replaced by W, almost the same creep properties, e.g., minimum creep rate, time to reach 2% strain and time for failure at 1123 and 1373 K, can be obtained [6]. Moreover, calculated thermal expansion coefficients and bulk moduli of γ'-Ni_3Al phases at finite temperature and certain pressure suggest that W is of potential possibility to replace Re in Ni-based SC superalloys [7]. However, for

Corresponding author: Ping PENG, Tel: +86-731-88821727, E-mail: ppeng@hnu.edu.cn
DOI: 10.1016/S1003-6326(21)65634-0

the flow behavior of γ'-Ni_3Al phases, these results don't provide how to be affected by partial replacements of W for Re. Therefore, a cooperative effect of duplex additions of Re and W on the dislocation slip mediated creep in γ'-Ni_3Al phases is desired.

Previous investigations showed that the configuration and movement of dislocations play an important role in the plastic deformation of γ' phases [8,9]. At the early stage of creep, the flow behavior of Ni-based SC superalloys mainly depends on the activation of 1/2⟨110⟩{111} dislocations in γ channels [10]. With the increase of dislocation densities in γ channels, some 1/2⟨110⟩{111} matrix pairs can combine to form ⟨110⟩{111} super dislocation at the γ/γ' interface. Once inside the γ' phase, these ⟨110⟩{111} super dislocations are easily dissociated [11]. At high temperature and low stress, the most possible deformation mechanism is to be sheared by 1/2⟨110⟩{111} pairs connected by an anti-phase boundary (APB) fault, i.e., ⟨110⟩{111} → 1/2⟨110⟩{111}+APB+1/2⟨110⟩{111} [12], and the 1/2⟨110⟩{111} super-partial dislocation can be further dissociated into two 1/6⟨112⟩{111} Shockley partial dislocations separated by a complex stacking fault (CSF), i.e., 1/2⟨110⟩{111}→ 1/6⟨112⟩{111}+CSF+1/6⟨112⟩{111} [12]. In this case, one ⟨110⟩{111} super dislocation can be described by four Shockley partial dislocations (i.e., P_1=P_3 and P_2=P_4) bounded by one APB and two CSFs (Fig. 1(a)), and a mutual elastic interaction among 1/2⟨110⟩{111} super-partial dislocations can generate a tangential force perpendicular to {111} slip plane [13]. In general, a high APB energy will make APB ribbons among 1/2⟨110⟩{111} super-partial dislocations narrow, leading to stronger tangential force and increased driving force of cross-slips of 1/2⟨110⟩{111} super-partial dislocations. It is widely accepted that this cross-slip of screw dislocations should be responsible for the anomalous flow behavior of γ' phases at high temperature [14]. For the cross-slip of 1/2⟨110⟩{111} dislocations, a temporary recombination of 1/6⟨112⟩{111} Shockley partial dislocations [13] is required, and a lifted CSF energy can lessen the width of CSF regions and lower the constriction energy of 1/6⟨112⟩{111} Shockley partial dislocations [14]. Owing to low APB energy in cubic {001} planes relative to octahedral {111} planes, Shockley partial dislocations P_3 and P_4 as a leading pair may cross-slip to {001} planes from {111} planes. As a result, Kear–Wilsdorf (K−W) lock [15] can be formed. This K−W lock will restrict the movement of P_3 and P_4, which makes Shockley partial dislocations P_1 and P_2 as a trailing pair stay still on {111} planes (Fig. 1(b)). Thus, the tendency of cross-slips of leading 1/2⟨110⟩{111} super-partial dislocations can be utilized to evaluate the ability of plastic deformations of γ' phases to some extent, and the easier the cross-slip of 1/2⟨110⟩{111} super-partial dislocations is, the larger the yield strength of γ' phases at high temperature is [16].

To obtain the information of dislocation slip mediated creeps, lots of researches on cross-slips of 1/2⟨110⟩{111} super-partial dislocations in γ' phases have been reported [13−15,17]. For example, the influence of refractory metals on generalized stacking fault energy curves (Γ-surfaces) [14,18] and ideal shear strengths (τ_{max}) [19,20] in $1/2[\bar{1}01](111)$ and $1/6[\bar{1}\,\bar{1}2](111)$ slip systems were

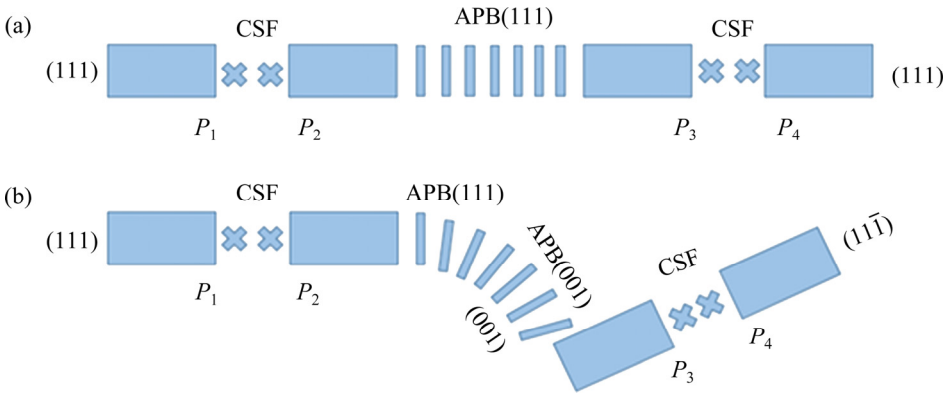

Fig. 1 Schematic diagrams of cross-slip of screw dislocations in $L1_2$-Ni_3Al crystals: (a) Before cross-slip; (b) After cross-slip

systematically investigated. It is pointed out that W-addition not only remarkably raises the APB energy γ_{APB} and CSF energy γ_{CSF} on (111) planes, but also hoists unstable stacking fault energies γ_{usf} and ideal shear strengths τ_{max}, and the magnitude is preceded only by Re in the sequence of Re>W>Mo>Ta>Ti>Ru, indicating that W-addition is beneficial to impeding the emission, propagation and movement of 1/2⟨110⟩{111} super-partial dislocations and 1/6⟨112⟩{111} Shockley partial dislocations. Moreover, it is demonstrated that the cross-slip activation enthalpy of 1/2⟨110⟩{111} super-partial dislocations can be lowered by the addition of Re, W and Mo [14], which means that W-addition may also accelerate the cross-slips and promote sessile dislocation locks to be generated, similarly to Re-addition. Recently, in the view of multi-component characteristics of Ni-based SC superalloys, a density functional theory (DFT) based cluster expansion calculation of composition-dependent γ_{APB} was also performed by DODARAN et al [13]. Their results showed that the impact of individual solute elements X on γ_{APB} obtained in a ternary $L1_2$-Ni_3Al(X) crystal cannot be directly translated to a multi-solute γ' phases due to a correlation and synergistic effect among solute elements. For this reason, the influence of multi-additions of Re and W on τ_{max} in $[\bar{1}10](111)$ and $[11\bar{2}](111)$ slip directions was further investigated [8,9]. It is found that a double Re-addition at preferential Al−Al sites may further elevate τ_{max} in the single Re-addition system, and τ_{max} in a multi-addition of Re and W is even larger than that of the double Re-addition, but an extra addition of Re or W at a Ni site is not conducive to the improvement of τ_{max} in $[\bar{1}10](111)$ and $[11\bar{2}](111)$ slip directions. This result once again indicates that the correlation and synergistic effect among solute elements cannot be ignored, and the interplay among refractory metals plays an important role in the dislocation slip mediated creeps of γ' phases.

In this work, several stacking fault models of $L1_2$-Ni_3Al(X) crystals with X=Re, W, Mo, Ta and Ti are constructed in order to investigate the interplay among refractory metals in APB and CSF in γ' phases. And then, exact calculations of Γ-surfaces and τ_{max} in $[\bar{1}10](111)$ and $[11\bar{2}](111)$ slip directions are carried out. Finally, the influence of various multiple additions on the cross-slip of 1/2⟨110⟩{111} super-partial dislocations and the nucleation and movement of 1/6⟨112⟩{111} Shockley partial dislocations is discussed, and a special attention is paid to the impact of a partial replacement of Re by W.

2 Calculation

The first-principles calculation is performed by Vienna *ab initio* simulation package (VASP) [21] based on the density functional theory (DFT), in which a plane-wave basis set with the projector augmented wave (PAW) [22] is used to characterize the ion−electron interaction, and the exchange correlation term is described within the generalized gradient approximation (GGA) parameterized by Perdew−Burke−Ernzerhof (PBE) functional [23]. In our self-consistent field (SCF) calculation, the cutoff energy of plane wave functions is set to be 350 eV. A conjugate gradient method [24] has been utilized to optimize the geometry and all atomic positions in the supercell are relaxed until the force on each atom is less than 0.009 eV/Å. The calculation of total energies and electronic structures is followed by cell optimization with SCF tolerance of 1×10^{-5} eV under GGA-PBE potential.

A series of 24-atom supercells have been constructed to calculate the ideal shear strength τ_{max} in $[\bar{1}10](111)$ and $[11\bar{2}](111)$ slip systems (Fig. 2(a)). Here, the shear direction $[\bar{1}10]$ or $[11\bar{2}]$ and the slip plane (111) have been rotated to be parallel to the lattice vector $\boldsymbol{a}$ and normal to the lattice vector $\boldsymbol{c}$ as proposed by ROUNDY et al [25] and OGATA et al [26], respectively. In the shear deformation, a particle swarm optimization algorithm [27] has been adopted to yield the curve of stress τ versus strain ε. After being sheared, the deformed lattice vectors $\boldsymbol{R}$ can be obtained by $\boldsymbol{R}=\boldsymbol{R}_0\boldsymbol{D}$, where the matrix $\boldsymbol{R}_0$ represents the un-deformed lattice vector. The deformation matrix $\boldsymbol{D}$ [19] is

$$\boldsymbol{D}=\begin{bmatrix}1 & 0 & 0\\ 0 & 1 & 0\\ \varepsilon & 0 & 1\end{bmatrix} \tag{1}$$

where ε is the shear strain, i.e., a ratio of displacement Δa with respect to height c in the rotated supercell. In the first-principles calculation, atom positions are represented by fractional coordinates. At each step of shear deformations, the

configuration of previous steps is used as a starting point [28]. The atom position and cell shape are relaxed under the constraint of fixed shear strain ε.

To calculate generalized stacking fault energy curves (Γ-surfaces) of $L1_2$-Ni_3Al crystals along $[\bar{1}10](111)$ and $[11\bar{2}](111)$ slip directions, several (111) surface models are also built by a similar redefined lattice method for the construction of aforementioned shear models. In these surface models, a slab model of 96 atoms is composed of 12 (111) atomic layers with the stacking sequence of ABCABCABCABC, and a 12 Å vacuum region is added in the direction normal to the slip plane to avoid the interaction among faults in two neighbor slabs (Fig. 2(b)). In the calculation of Γ-surfaces, the atoms over a designated (111) slip plane will be moved along the $[\bar{1}10]$ or $[11\bar{2}]$ direction. As a result of shearing $b=a_0/2$ in the $[\bar{1}10](111)$ direction and $b=a_0/6$ in the $[11\bar{2}](111)$ direction, an anti-phase boundary (APB) fault and complex stacking fault (CSF) will be generated, respectively. As for the calculation of Γ-surfaces of APBs on a (001) plane, the surface model is shown in Fig. 2(c). Its APB can be obtained by slipping a part of atoms over a designated (001) slip plane along [110] direction until a distance $b=a_0/2$, in which a_0 is an equilibrium lattice parameter of $L1_2$-Ni_3Al crystals. In the movement of slabs, all atoms in the supercell will be relaxed, but only the direction perpendicular to (111) or (001) plane is allowed.

3 Results and discussion

3.1 Effect of alloying elements on dislocation slip mediated creep of γ' phases

Previous investigations [29−31] revealed most of Ta and Ti partition to the γ' phase, while W uniformly distributes between the γ matrix and γ' precipitates. Re and Mo mainly partition to the γ phase, but some of them enable to enter into γ' phases [18]. In the γ'-Ni_3Al phase, either Ta and Ti or W, Re and Mo preferentially occupy Al sites [31,32]. As one Al atom on the (111) slip plane is substituted by X=Ta, Ti, W, Re, Mo (marked as X_{Al}), the Γ-surfaces along $[\bar{1}10](111)$ and $[11\bar{2}](111)$ slip directions in γ'-$Ni_3Al(X)$ phases are calculated firstly. From Figs. 3(a, b), one can see that the APB energy γ_{APB}^{111} and the CSF energy γ_{CSF}

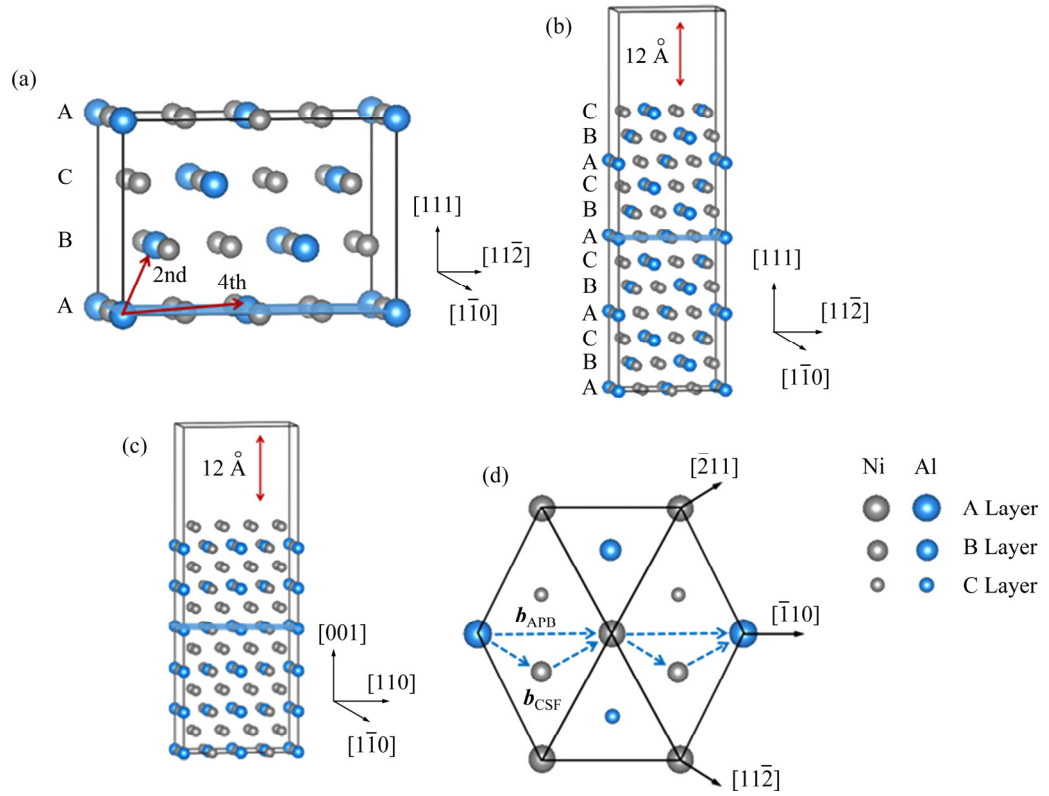

Fig. 2 Schematic diagrams of $Ni_3Al(X)$ stacking fault models for calculation of τ_{max} and Γ-surfaces: (a) τ_{max}; (b) Γ-surfaces of (111) plane; (c) Γ-surfaces of (001) plane; (d) Burger's vectors $\boldsymbol{b}_{APB}$ and $\boldsymbol{b}_{CSF}$ corresponding to APB and CSF (The shadow areas denote (111) or (001) slip planes; Grey and blue balls stand for Ni and Al atoms, respectively)

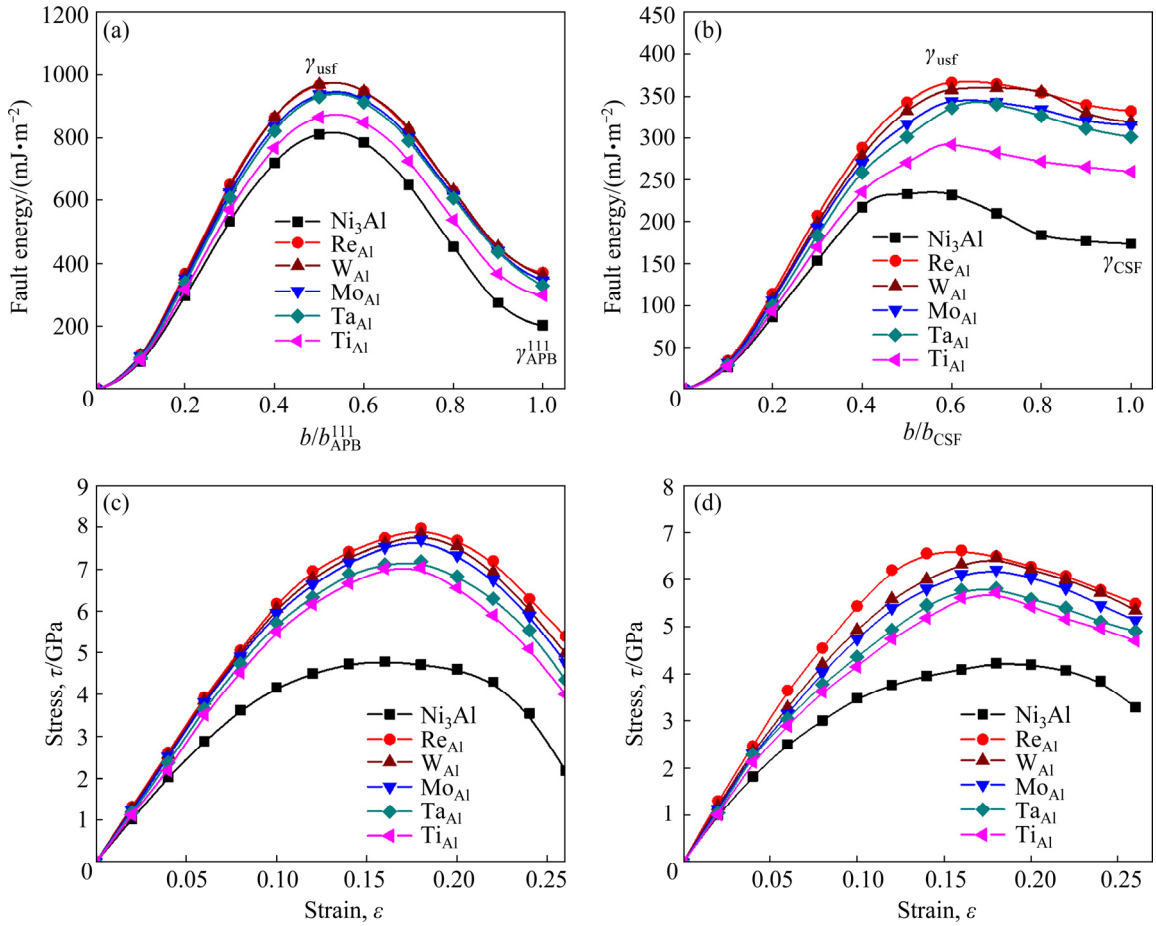

Fig. 3 Curves of fault energy (a, b) and stress τ vs strain ε (c, d) in $Ni_3Al(X)$ stacking fault models: (a, c) $[\bar{1}10](111)$ slip direction; (b, d) $[11\bar{2}](111)$ slip direction

in a perfect $L1_2$-Ni_3Al crystal are 203 and 173 mJ/m^2, respectively. These values agree well with previous calculation results [14]. As for single X-addition, Fig. 3(a) shows γ_{APB}^{111} (=371 mJ/m^2) in the Re_{Al} model is the largest, and then γ_{APB}^{111} (=362 mJ/m^2) in the W_{Al} model and γ_{APB}^{111} (=346 mJ/m^2) in the Mo_{Al} model, followed by γ_{APB}^{111} (=329 mJ/m^2) in the Ta_{Al} model and γ_{APB}^{111} (=299 mJ/m^2) in the Ti_{Al} model. As well known, γ_{APB}^{111} strongly affects the cross-slip of 1/2⟨110⟩{111} super-partial dislocations. As γ_{APB}^{111} is low, the tangential force component generated by the interaction of 1/2⟨110⟩{111} super-partial dislocations may significantly reduce cross-slip rate [13]. Obviously, all of Ta-, Ti-, W-, Re- and Mo-addition can improve the cross-slip of 1/2⟨110⟩{111} super-partial dislocations from {111} to {001} planes, among which the Re-addition is the best. Meanwhile, a similar variation of γ_{CSF} to γ_{APB}^{111} can also be observed from Fig. 3(b). That is: γ_{CSF} (=332 mJ/m^2) in Re_{Al} model > γ_{CSF} (=319 mJ/m^2) in W_{Al} model > γ_{CSF} (=315 mJ/m^2) in Mo_{Al} model > γ_{CSF} (=301 mJ/m^2) in Ta_{Al} model > γ_{CSF} (=260 mJ/m^2) in Ti_{Al} model. Since γ_{CSF} determines the driving force of cross-slips to some extent and affects the width of two CSF regions related to the energy of constrictions of 1/6⟨112⟩{111} Shockley partial dislocations [14], an increasing γ_{CSF} relative to the perfect $L1_2$-Ni_3Al crystal indicates that Re-, W-, Mo-, Ta- and Ti-addition can also decrease the width of CSF regions. Therefore, they can all lower the constriction energy of 1/6⟨112⟩{111} Shockley partial dislocations.

The unstable stacking fault energy γ_{usf} [33−35], as a measure of energy release rate for dislocation nucleation relevant to ductile response of the material, represents an intrinsic energy barrier for activated stacking faults. In the separation of ⟨110⟩{111} super dislocations, a high γ_{usf} means a large shear stress to be requested for the nucleation of 1/2⟨110⟩{111} super-partial dislocations [18]. Figures 3(a, b) show that γ_{usf} values in $[\bar{1}10](111)$ and $[11\bar{2}](111)$ slip directions are simultaneously

elevated by single X-addition. For example, relative to the perfect $L1_2$-Ni_3Al crystal, γ_{usf} in $[\bar{1}10](111)$ and $[11\bar{2}](111)$ slip directions are lifted by 162 and 159 mJ/m^2 in the Re-addition model, respectively. These results indicate that either emission of 1/2⟨110⟩{111} super-partial dislocations or nucleation of 1/6⟨112⟩{111} Shockley partial dislocations is restricted by Re-, W-, Mo-, Ta- and Ti-addition, and the order of Re_{Al}>W_{Al}>Mo_{Al}>Ta_{Al}> Ti_{Al}>Ni_3Al reveals that Suzuki segregations [36,37] of Re, W, Mo at APBs and CSFs are more profitable than the partitioning of Ta and Ti in γ' phases.

Another parameter related to γ_{usf} is the ideal shear strength τ_{max}, which is a critical stress required to plastically deform a perfect crystal [26]. τ_{max} provides an upper bound of creep strength a material can achieve [28], although it can be affected by dislocations, grain boundaries, cracks and other micro-structural defects in a real crystal. To obtain some crucial information of resistances to creep deformations, τ_{max} in $[\bar{1}10](111)$ and $[11\bar{2}](111)$ slip systems are further calculated. Figures 3(c, d) exhibit the variation of stress τ versus strain ε in the γ'-Ni_3Al(X) phase with and without single X-addition. For the perfect $L1_2$-Ni_3Al crystal, Fig. 3(c) shows that the shear stress τ along $[\bar{1}10]$ direction reaches its maximum value of 4.79 GPa at ε=0.16, which means that τ_{max} in the $[\bar{1}10](111)$ slip direction is 4.79 GPa. Similarly, τ_{max} (=4.23 GPa) at ε=0.18 in the $[11\bar{2}](111)$ slip direction can also be deduced from Fig. 3(d). In Re_{Al}, W_{Al}, Mo_{Al}, Ta_{Al} and Ti_{Al} models, τ_{max} is found to increase by 3.17, 3.04, 2.90, 2.39 and 2.25 GPa in the $[\bar{1}10](111)$ slip direction and 2.39, 2.24, 1.98, 1.58 and 1.49 GPa in the $[11\bar{2}](111)$ slip direction relative to the perfect $L1_2$-Ni_3Al crystal, respectively, which means that all of Re, W, Mo, Ta and Ti can act as an efficient obstacle in the movement of initial 1/2⟨110⟩{111} super-partial dislocations and subsequent 1/6⟨112⟩{111} Shockley partial dislocations. Consequently, from the resistance to dislocation movements concerned, Re-, W-, Mo-, Ta- and Ti-additions are also profitable for the improvement of creep strengths of Ni-based SC superalloys.

Since the anomalous flow behavior of $L1_2$-Ni_3Al crystals at high temperature mainly arises from thermally activated cross-slips of screw dislocations from primary {111} slip planes onto the {001} cubic planes, a variation of configuration energies of ⟨110⟩{111} super dislocations induced by cross-slips of 1/2⟨110⟩{111} super-partial dislocations is further calculated on the basis of PPV model (Fig. 1). In this PPV model [38], the difference in configuration energies of super dislocations per unit length before and after cross-slips can be evaluated by

$$\Delta E=\left(\gamma_{APB}^{001}-\frac{\gamma_{APB}^{111}}{\sqrt{3}}\right)\cdot w \tag{2}$$

where γ_{APB}^{001} is APB energy in {001} stacking faults, and w is the distance of cross-slips from {111} to {001} planes.

Obviously, the cross-slip of 1/2⟨110⟩{111} super-partial dislocations can take place only if $\gamma_{APB}^{111}/\gamma_{APB}^{001}>\sqrt{3}$. A large $\gamma_{APB}^{111}/\gamma_{APB}^{001}$ means that γ' phases have a higher driving force of 1/2⟨110⟩{111} super-partial dislocations from {111} to {001} planes. In this case, some K−W locks [16] are easy to be formed with the help of APBs on {001} planes. To this end, we employ $\gamma_{APB}^{111}/\gamma_{APB}^{001}$ to evaluate the influence of single X-addition on the yield strength of γ' phases at high temperature. The calculated results are tabulated in Table 1. From Table 1, one can see that $\gamma_{APB}^{111}/\gamma_{APB}^{001}$(=1.84>$\sqrt{3}$) in the perfect $L1_2$-Ni_3Al crystal indeed complies with the condition of cross-slips of 1/2⟨110⟩{111} super-partial dislocations as reported in literatures [17]. As a part of Al atoms in γ'-Ni_3Al(X) phases are substituted by Re, W and Mo, $\gamma_{APB}^{111}/\gamma_{APB}^{001}$ values are found to increase by 0.18, 0.16 and 0.09, respectively, while only a small rise can be seen in the case of X=Ta and Ti, e.g., 0.05 in the Ta_{Al} model and 0.03 in the Ti_{Al} mode. These results clearly indicate that Re- and W-additions can remarkably promote the cross-slip of 1/2⟨110⟩{111} super-partial dislocations, but Ta- and Ti-additions are almost invalid. As for the advantage of Suzuki segregations, a careful comparison reveals that either $\gamma_{APB}^{111}/\gamma_{APB}^{001}$ associated with anomalous yield strength of γ' phases at high temperature or τ_{max} relevant to resistances to plastic deformations of γ' phases in the W-addition model is almost equal to that in the Re-addition model. For example, for the substitution of W for Al in γ'-Ni_3Al(X) phases, Table 1 shows that τ_{max} (=6.47 GPa) in the $[11\bar{2}](111)$ slip direction is very close to that (=6.62 GPa) in the single Re-addition model. These results seem to imply that W-addition indeed has a

Table 1 Formation enthalpies of point defects H, correlation energies $\Delta E^{X1_{Al}+X2_{Al}}(d)$ between $X1_{Al}$ and $X2_{Al}$ defects, ideal shear strengths τ_{max}, anti-phase boundary energies γ_{APB}, complex stacking fault energies γ_{CSF}, unstable stacking fault energies γ_{usf} and $\gamma_{APB}^{111}/\gamma_{APB}^{001}$ in γ'−Ni_3Al(X) phases with X=Re, W, Mo, Ta and Ti

Model	H/eV	$\Delta E^{X1_{Al}+X2_{Al}}(d)$/eV	$[\bar{1}10](111)$			$[11\bar{2}](111)$			$[110](001)$	$\gamma_{APB}^{111}/\gamma_{APB}^{001}$
			τ_{max}/GPa	γ_{usf}/(mJ·m^{-2})	γ_{APB}^{111}/(mJ·m^{-2})	τ_{max}/GPa	γ_{usf}/(mJ·m^{-2})	γ_{CSF}/(mJ·m^{-2})	γ_{APB}^{001}/(mJ·m^{-2})	
Ni_3Al			4.79	811	203	4.23	233	173	110	1.84
Re_{Al}	0.910		7.96	973	371	6.62	366	332	183	2.02
W_{Al}	0.551		7.83	970	362	6.47	360	319	181	2.00
Mo_{Al}	0.794		7.69	937	346	6.21	344	315	179	1.93
Ta_{Al}	−0.240		7.18	931	329	5.81	340	301	174	1.89
Ti_{Al}	−0.358		7.04	866	299	5.72	292	260	160	1.87
$M_{Re_{Al}}^{Re_{Al}}$(2nd)	1.940	0.120	8.30	1023	351	6.90	428	406	162	2.16
$M_{Re_{Al}}^{Re_{Al}}$(4th)	1.905	0.085	8.61	1097	481	7.63	449	396	198	2.43
$M_{W_{Al}}^{Re_{Al}}$(2nd)	1.558	0.097	8.64	1058	416	7.36	479	426	202	2.06
$M_{W_{Al}}^{Re_{Al}}$(4th)	1.536	0.075	8.99	1115	543	7.70	493	369	228	2.38
$M_{Mo_{Al}}^{Re_{Al}}$(2nd)	1.844	0.140	8.42	1025	384	7.20	461	390	216	1.78
$M_{Mo_{Al}}^{Re_{Al}}$(4th)	1.799	0.095	8.68	1081	505	7.59	477	335	260	1.94
$M_{Ta_{Al}}^{Re_{Al}}$(2nd)	0.781	0.111	8.56	1046	445	7.36	473	436	220	2.02
$M_{Ta_{Al}}^{Re_{Al}}$(4th)	0.747	0.077	8.92	1085	556	7.51	488	423	255	2.18
$M_{Ti_{Al}}^{Re_{Al}}$(2nd)	0.742	0.190	8.44	1002	399	7.09	433	365	213	1.88
$M_{Ti_{Al}}^{Re_{Al}}$(4th)	0.671	0.119	8.67	1031	480	7.23	440	363	250	1.91
$M_{Mo_{Al}}^{W_{Al}}$(2nd)	1.326	−0.019	8.73	1049	502	7.46	476	440	225	2.22
$M_{Mo_{Al}}^{W_{Al}}$(4th)	1.287	−0.058	8.95	1095	607	7.53	488	432	260	2.33
$M_{Ta_{Al}}^{W_{Al}}$(2nd)	0.375	0.064	8.83	1054	452	7.37	485	476	230	1.96
$M_{Ta_{Al}}^{W_{Al}}$(4th)	0.339	0.028	9.12	1097	462	7.50	490	483	260	2.16
$M_{Ti_{Al}}^{W_{Al}}$(2nd)	0.329	0.136	8.42	1010	441	6.86	436	388	244	1.81
$M_{Ti_{Al}}^{W_{Al}}$(4th)	0.278	0.085	8.62	1036	516	7.14	437	400	275	1.88
$M_{Ta_{Al}}^{Mo_{Al}}$(2nd)	0.545	−0.009	8.59	1026	460	7.21	456	438	211	2.18
$M_{Ta_{Al}}^{Mo_{Al}}$(4th)	0.503	−0.051	8.93	1062	567	7.34	485	448	245	2.31
$M_{Ti_{Al}}^{Mo_{Al}}$(2nd)	0.397	−0.039	8.18	1010	401	6.73	426	353	211	1.90
$M_{Ti_{Al}}^{Mo_{Al}}$(4th)	0.346	−0.090	8.38	1039	479	6.98	444	372	247	1.94
$M_{Ti_{Al}}^{Ta_{Al}}$(2nd)	−0.461	0.137	7.79	972	438	6.45	412	366	216	2.03
$M_{Ti_{Al}}^{Ta_{Al}}$(4th)	−0.495	0.103	7.99	998	497	6.66	445	409	243	2.05

similar influence to Re-addition on the creep of Ni-based SC superalloys at high temperature [9].

3.2 Comparison of strengthening effects caused by W-addition with Re-addition

As it is well-known, Re-addition induced reinforcement of creep resistances in Ni-based SC superalloys is called as Re-effect [4]. Re not only may reduce stacking fault energies of γ phases and raise γ_{APB}^{111} of γ' phases, but also can slow down coarsening kinetics of γ' precipitates [39]. Since almost same creep properties have been observed in

CMSX-4 superalloys with partial substitution of W for Re [6], a multiple addition of Re and W in γ' phases is further investigated. In these complexes of $X1_{Al}$+$X2_{Al}$ defects, only two typical models $M^{X1_{Al}}_{X2_{Al}}$(2nd) and $M^{X1_{Al}}_{X2_{Al}}$(4th) with preferred substitution of X1 and X2 for Al atoms are calculated. The calculated results are also listed in Table 1. Herein, X1 and X2 represent the species of alloying elements. *d*=2nd and *d*=4th are the distances between $X1_{Al}$ and $X2_{Al}$ point defects, which correspond to the second and fourth nearest neighbors of assigned sites (Fig. 2(a)), respectively. From Fig. 2(a), one can see that *d*=2nd denotes that $X2_{Al}$ locates at an adjacent plane of the assigned (111) slip plane, while *d*=4th means that $X2_{Al}$ situates at the same (111) slip planes as $X1_{Al}$. The former indicates that only Suzuki segregation of X1 exists, but the latter means that co-segregation of X1 and X2 appears in these stacking faults. Corresponding to X_{Al} and $X1_{Al}$+$X2_{Al}$, the contents of solutes in the shear models are 4.17 and 8.33 at.%, while they are 1.04 and 2.08 at.% in the calculation models for Γ-surfaces, respectively. Relative to the single Re-addition, Table 1 shows that $\gamma^{111}_{APB}/\gamma^{001}_{APB}$ in $M^{Re_{Al}}_{Re_{Al}}$(2nd) and $M^{Re_{Al}}_{Re_{Al}}$(4th) models rises by 7% and 20%, respectively, and τ_{max} in the $[11\bar{2}](111)$ slip direction increases by 0.28 and 1.01 GPa, respectively. Obviously, an extra Re-addition is conducive to yield strengths and creep rupture strengths of γ' phases at high temperature [8], especially in the Suzuki segregation of Re with high concentration. As X2 is replaced by W, it is found that both of γ_{usf} in $[\bar{1}10](111)$ and $[11\bar{2}](111)$ slip directions are large relative to their corresponding double Re-addition models, which means that a partial replacement of W for Re makes the emission of $1/2\langle 110\rangle\{111\}$ super-partial dislocations and the nucleation of $1/6\langle 112\rangle\{111\}$ Shockley partial dislocations more difficult [18], and the inhibition caused by W-segregation on the (111) slip plane is stronger than W-addition on its adjacent plane, e.g., 57 mJ/m^2 in the $M^{Re_{Al}}_{W_{Al}}$(4th) model larger than that in the $M^{Re_{Al}}_{W_{Al}}$(2nd) model, corresponding to the emission of $1/2\langle 110\rangle\{111\}$ super-partial dislocations. Moreover, an upraised γ_{CSF} in the complex of Re_{Al}+W_{Al} indicates that the substitution of Re by W also facilitates the constriction of $1/2\langle 110\rangle\{111\}$ super-partial dislocations by two $1/6\langle 112\rangle\{111\}$ Shockley partial dislocations [14]. Additionally, relative to the double Re-addition with *d*=2nd and *d*=4th, τ_{max} in the $[11\bar{2}](111)$ slip direction increases by 0.46 and 0.07 GPa, respectively, which means that both of replacements of W for Re on the (111) slip plane and its adjacent plane can significantly impede the movement of $1/6\langle 112\rangle\{111\}$ Shockley partial dislocations, and its resistance to dislocation slip mediated creeps of γ' phases seems to be large relative to double Re-additions. But, it is noticed that $\gamma^{111}_{APB}/\gamma^{001}_{APB}$ in $M^{Re_{Al}}_{W_{Al}}$(2nd) and $M^{Re_{Al}}_{W_{Al}}$(4th) models drops by 4% and 2% relative to $M^{Re_{Al}}_{Re_{Al}}$(2nd) and $M^{Re_{Al}}_{Re_{Al}}$(4th) models, respectively. From the viewpoint of cross-slips of $1/2\langle 110\rangle\{111\}$ super-partial dislocations, this reduced $\gamma^{111}_{APB}/\gamma^{001}_{APB}$ undoubtedly indicates that the anomalous flow behavior of γ' phases at high temperature in Re_{Al}+W_{Al} complexes is not as excellent as that of the double Re-addition.

As X1 on the (111) slip plane is also replaced by W, Table 1 shows although most of $\gamma^{111}_{APB}/\gamma^{001}_{APB}$ and τ_{max} in the $[11\bar{2}](111)$ slip direction are lower than those in Re_{Al}+$X2_{Al}$ complexes, their decrements are found to be very small. For example, relative to the $M^{Re_{Al}}_{Ta_{Al}}$(4th) model, only 0.01 GPa is cut down for τ_{max}, and the lost $\gamma^{111}_{APB}/\gamma^{001}_{APB}$ is less than 1% in the $M^{W_{Al}}_{Ta_{Al}}$(4th) model. Moreover, a similar variation can also be seen as X2 departs from the (111) slip plane. For example, τ_{max} (=7.37 GPa) in the $M^{W_{Al}}_{Ta_{Al}}$(2nd) model is very close to that (7.36 GPa) in the $M^{Re_{Al}}_{Ta_{Al}}$(2nd) model, and their corresponding difference in $\gamma^{111}_{APB}/\gamma^{001}_{APB}$ is not more than 0.06. These results clearly indicate that W-addition indeed has a similar strengthening effect to Re-addition on the dislocation slip mediated creep of γ' phases, especially in the co-segregation of W and Mo. Interestingly, for the complex of W_{Al}+Mo_{Al}, it is found that either $\gamma^{111}_{APB}/\gamma^{001}_{APB}$=2.22 at *d*=2nd or $\gamma^{111}_{APB}/\gamma^{001}_{APB}$=2.33 at *d*=4th is higher than that in the $M^{Re_{Al}}_{Mo_{Al}}$(2nd) model (1.78) and that in the $M^{Re_{Al}}_{Mo_{Al}}$(4th) model (1.94). This result further indicates that an interplay between X1 and X2 has a more critical impact than their species on the anomalous flow behavior of γ' phases.

To investigate the interplay between X1 and X2 in dislocation slip mediated creeps of γ' phases, a correlation energy function $\Delta E^{X1_{Al}+X2_{Al}}(d)$ has been adopted to characterize and assess the interaction between $X1_{Al}$ and $X2_{Al}$ point defects

(Table 1). Herein, $\Delta E^{X1_{Al}+X2_{Al}}(d)$ is a difference of formation enthalpies of point defects, which can be calculated by the following expression [40]:

$$\Delta E^{X1_{Al}+X2_{Al}}(d)=H_{X1_{Al}+X2_{Al}}(d)-H_{X1_{Al}}-H_{X2_{Al}} \quad (3)$$

where $H_{X1_{Al}}$, $H_{X2_{Al}}$ and $H_{X1_{Al}+X2_{Al}}(d)$ are the formation enthalpies of $L1_2$-$Ni_3Al(X)$ crystals per atom, corresponding to $X1_{Al}$, $X2_{Al}$ and $M^{X1_{Al}}_{X2_{Al}}(d)$ models, respectively. Table 1 shows that almost all $\Delta E^{X1_{Al}+X2_{Al}}(d)$ in $M^{X1_{Al}}_{X2_{Al}}(d)$ models are positive, e.g., $\Delta E^{X1_{Al}+X2_{Al}}(d)=0.085$ eV in the $M^{Re_{Al}}_{Re_{Al}}(4th)$ model and $\Delta E^{X1_{Al}+X2_{Al}}(d)=0.075$ eV in the $M^{Re_{Al}}_{W_{Al}}(4th)$ model, which means that most of interactions between $X1_{Al}$ and $X2_{Al}$ point defects are repulsive forces. However, it is noticed that a negative $\Delta E^{X1_{Al}+X2_{Al}}(d)=-0.058$ eV exists in the $M^{W_{Al}}_{Mo_{Al}}(4th)$ model, indicating that the interaction between W_{Al} and Mo_{Al} point defects is attractive. As compared with $\Delta E^{X1_{Al}+X2_{Al}}(d)=0.095$ eV in the $M^{Re_{Al}}_{Mo_{Al}}(4th)$ model, this negative interaction seems to imply that an attraction should be responsible for a large $\gamma^{111}_{APB}/\gamma^{001}_{APB}$ in the $M^{W_{Al}}_{Mo_{Al}}(4th)$ model relative to the $M^{Re_{Al}}_{Mo_{Al}}(4th)$ model. To test and verify this conjecture, $\Delta E^{X1_{Al}+X2_{Al}}(d)$ in the complexes of Mo_{Al}+Ta_{Al}, Mo_{Al}+Ti_{Al} and Ta_{Al}+Ti_{Al} as well as their $\gamma^{111}_{APB}/\gamma^{001}_{APB}$ and τ_{max} are also calculated and listed in Table 1. From Table 1, one can see that relative to $M^{Re_{Al}}_{Ta_{Al}}(4th)$ and $M^{W_{Al}}_{Ta_{Al}}(4th)$ models, $\gamma^{111}_{APB}/\gamma^{001}_{APB}$ indeed increases in the $M^{Mo_{Al}}_{Ta_{Al}}(4th)$ model with negative $\Delta E^{X1_{Al}+X2_{Al}}(d)$. Also, $\gamma^{111}_{APB}/\gamma^{001}_{APB}$ in $M^{Mo_{Al}}_{Ti_{Al}}(4th)$ model with $\Delta E^{X1_{Al}+X2_{Al}}(d)=-0.080$ eV rises by 0.03 and 0.06 eV, respectively, compared with $M^{Re_{Al}}_{Ti_{Al}}(4th)$ and $M^{W_{Al}}_{Ti_{Al}}(4th)$ models with positive $\Delta E^{X1_{Al}+X2_{Al}}(d)$. As for the influence of magnitudes of $\Delta E^{X1_{Al}+X2_{Al}}(d)$, Fig. 4 further illustrates the variation of $\gamma^{111}_{APB}/\gamma^{001}_{APB}$ and τ_{max} versus $\Delta E^{X1_{Al}+X2_{Al}}(d)$. For d=2nd, one can see that with the increase of $\Delta E^{X1_{Al}+X2_{Al}}(2nd)$ from −0.039 to 0.190 eV, both of $\gamma^{111}_{APB}/\gamma^{001}_{APB}$ and τ_{max} in the $[11\bar{2}](111)$ slip direction ascend firstly, and then gradually fall down, and the transformation takes place at $\Delta E^{X1_{Al}+X2_{Al}}(2nd)\approx 0.050$ eV. In the case of d=4th, a similar variation of $\gamma^{111}_{APB}/\gamma^{001}_{APB}$ and τ_{max} versus $\Delta E^{X1_{Al}+X2_{Al}}(4th)$ can be seen with the increase of $\Delta E^{X1_{Al}+X2_{Al}}(4th)$ from −0.090 to 0.119 eV. Also, the largest $\gamma^{111}_{APB}/\gamma^{001}_{APB}$ and τ_{max} emerge at 0.050 eV, although their drop is more abrupt after the maximum. Similar to the influence of Re−P pairs on the Griffith work of γ-Ni/γ'-Ni_3Al interfaces [41], these results distinctly indicate that a weak interaction between $X1_{Al}$ and $X2_{Al}$ defects is more profitable for the improvement of creep strengths of γ' phases at high temperature, and the smaller the magnitude of $\Delta E^{X1_{Al}+X2_{Al}}(d)$ is, the larger the creep rupture strength of γ'-Ni_3Al phases is. That is said, the anomalous flow behavior of γ' phases at high temperature cannot benefit from a strong interaction between $X1_{Al}$ and $X2_{Al}$ defects regardless of attraction or repulsion. Thus, relative to the species of X1 and X2 and their defective configurations in γ' phases, $\Delta E^{X1_{Al}+X2_{Al}}(d)$ provides a simple and direct criterion for the estimation of yield strengths and creep rupture strengths of γ' phases at high temperature to some extent.

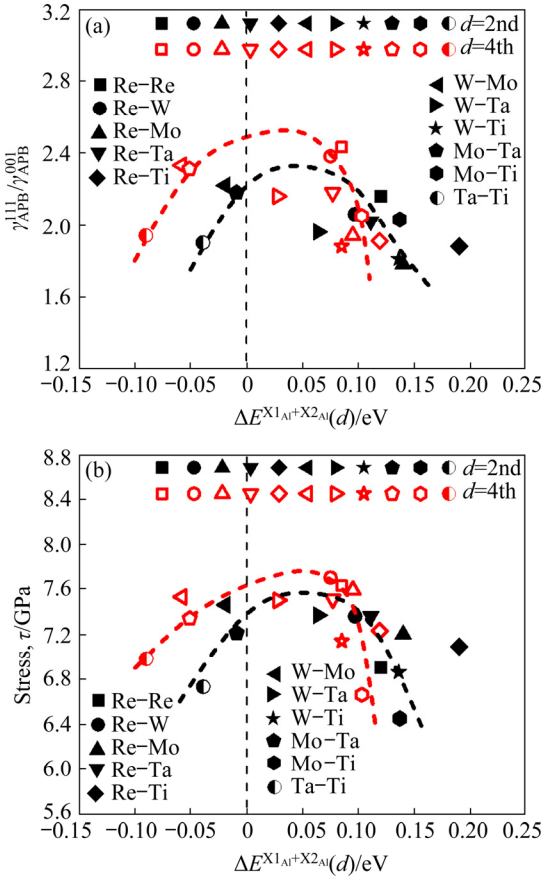

Fig. 4 Dependence of $\gamma^{111}_{APB}/\gamma^{001}_{APB}$ (a) and τ_{max} in $[11\bar{2}](111)$ slip direction (b) on $\Delta E^{X1_{Al}+X2_{Al}}(d)$ in complex of $X1_{Al}$ and $X2_{Al}$

4 Conclusions

(1) Similar to Re-addition, the Suzuki

segregation of W at {111} stacking faults not only can impede the movement of 1/6⟨112⟩{111} Shockley partial dislocations, but also may promote the cross-slip of 1/2⟨110⟩{111} super-partial dislocations.

(2) With the partial replacement of W for Re, an increased τ_{max} along the $[11\bar{2}](111)$ slip direction in the duplex addition model of Re and W suggests that the resistance to creep of γ' phases can be reinforced, although their $\gamma_{APB}^{111}/\gamma_{APB}^{001}$ associated with the anomalous flow behavior of γ' phases drops slightly.

(3) The anomalous flow behavior of γ' phases at high temperature can benefit from the co-segregation of Re and W in {111} stacking faults, but a strong attraction and repulsion between $X1_{Al}$ and $X2_{Al}$ point defects are disadvantageous for the improvement of creep rupture strengths of Ni-based single crystal superalloys.

Acknowledgments

The authors are grateful for the financial supports from the National Natural Science Foundation of China (Nos. 51871096, 52071136).

References

[1] REED R C. The superalloys fundamentals and applications [M]. Cambridge: Cambridge University Press, 2006.

[2] LONG Hai-bo, MAO Sheng-cheng, LIU Yi-nong, ZHANG Ze, HAN Xiao-dong. Microstructural and compositional design of Ni-based single crystalline superalloys—A review [J]. Journal of Alloys and Compounds, 2018, 743: 203−220.

[3] HUANG Yan-yan, MAO Zu-gang, NOEBE R D, SEIDMAN D N. The effects of refractory elements on Ni-excesses and Ni-depletions at γ(f.c.c.)/γ'($L1_2$) interfaces in model Ni-based superalloys: Atom-probe tomographic experiments and first-principles calculations [J]. Acta Materialia, 2016, 121: 288−298.

[4] ERICKSON G L. The development and application of CMSX-10 [J]. Superalloys, 1996, 1: 35−44.

[5] RAE C M F, REED R C. The precipitation of topologically close-packed phases in rhenium containing superalloys [J]. Acta Materialia, 2001, 49: 4113−4125.

[6] WOLLMER S, MACK T, GLATZELl U. Influence of tungsten and rhenium concentration on creep properties of a second generation superalloy [J]. Materials Science and Engineering A, 2001, 321: 792−795.

[7] GONG Wei, ZHAO Wen-yue, MIAO Nai-hua, SUN Zhi-mei, LI Shu-suo, GONG Sheng-kai. Strengthening effects of alloying elements W and Re on Ni_3Al: A first-principles study [J]. Computational Materials Science, 2018, 144: 23−31.

[8] CHEN Yi, HE Shuang, YI Zhou, PENG Ping. Impact of correlative defects induced by double Re-addition on the ideal shear strength of γ'-Ni_3Al phases [J]. Computational Materials Science, 2018, 152: 408−416.

[9] CHEN Yi, HE Shuang, YI Zhou, PENG Ping. A synergistic reinforcement of Re and W for ideal shear strengths of γ'-Ni_3Al phases [J]. Journal of Physics and Chemistry of Solids, 2019, 131: 34−43.

[10] LV Xian-zi, ZHANG Jian-xin. Core structure of a ⟨100⟩ interfacial superdislocations in a nickel-base superalloy during high-temperature and low-stress creep [J]. Materials Science and Engineering A, 2017, 683: 9−14.

[11] LIU Li-rong, JIN Tao, ZHAO Nai-ren, WANG Zi-hui, SUN Xiao-feng, GUAN Heng-rong, HU Zhuang-qi. Creep deformation mechanism in a Ni base single crystal superalloy [J]. Acta Metallurgica Sinica, 2005, 41: 1215−1220.

[12] MILLIGAN W W, ANTOLOVICH S D. The mechanisms and temperature dependence of superlattice stacking fault formation in the single-crystal superalloy PWA 1480 [J]. Metallurgical Transactions A, 1990, 22: 2309−2318.

[13] DODARAN M, ETTEFAGH A H, GUO S M, KHONSARI M M, MENG W J, SHAMSAEI N, SHAO S. Effect of alloying elements on the γ' antiphase boundary energy in Ni-base superalloys [J]. Intermetallics, 2020, 117: 106670.

[14] YU Xiao-xiang, WANG Chong-yu. Effect of alloying element on dislocation cross-slip in γ'-Ni_3Al: A first-principles study [J]. Philosophical Magazine, 2012, 92: 4028−4039.

[15] WANG K Y M. Understanding the yield behaviour of $L1_2$-ordered alloys [J]. Materials Science and Technology, 2016, 33: 934−943.

[16] YOO M H. On the theory of anomalous yield behavior of Ni_3Al−Effect of elastic anisotropy [J]. Scripta Metallurgica, 1986, 20: 915−920.

[17] SHANG Shun-li, SHIMANEK J, QIN Shi-pin, WANG Yi, BEESE A M, LIU Zi-kui. Unveiling dislocation characteristics in Ni_3Al from stacking fault energy and ideal strength: A first-principles study via pure alias shear deformation [J]. Physical Review B, 2020, 101: 024102.

[18] YU Xiao-xiang, WANG Chong-yu. The effects of alloying elements on generalized stacking fault energies, strength and ductility of γ'-Ni_3Al [J]. Materials Science and Engineering A, 2012, 539: 38−41.

[19] WANG Yu-jiang, WANG Chong-yu. Influence of the alloying element Re on the ideal tensile and shear strength of γ'-Ni_3Al [J]. Scripta Materialia, 2009, 61: 197−200.

[20] WU Xiao-xia, WANG Chong-yu. Effect of the alloying element on the temperature-dependent ideal shear strength of γ'-Ni_3Al [J]. RSC Advances, 2016, 6: 20551−20558.

[21] KRESSE G, HAFNER J. Ab initio molecular dynamics for liquid metals [J]. Physical Review B, 1993, 47: 558−561.

[22] KRESSE G, JOUBERT D. From ultrasoft pseudopotentials to the projector augmented-wave method [J]. Physical Review B, 1999, 59: 1758−1775.

[23] PERDEW J P, BURKE K, ERNZERHOF M. Generalized gradient approximation made simple [J]. Physical Review Letters, 1996, 77: 3865−3868.

[24] HESTENES M R, STIEFEL E. Methods of conjugate

gradients for solving linear systems [J]. Journal of Research of the National Bureau Standards, 1952, 49: 409−436.
[25] ROUNDY D, KRENN C R, COHEN M L, MORRIS J J W. Ideal shear strengths of fcc aluminum and copper [J]. Physical Review Letters, 1999, 82: 2713−2716.
[26] OGATA S, LI J, YIP S. Ideal pure shear strength of Aluminum and Copper [J]. Science, 2002, 298: 807−811.
[27] LI Quan, LIU Han-yu, ZHOU Dan, ZHENG Wei-tao, WU Zhi-jian, MA Yan-ming. A novel low compressible and superhard carbon nitride: Body-centered tetragonal CN_2 [J]. Physical Chemistry Chemical Physics, 2012, 14: 13081−13087.
[28] JAHNATEK M, HAFNER J, KRAJCI M. Shear deformation, ideal strength, and stacking fault formation of fcc metals: A density-functional study of Al and Cu [J]. Physical Review B, 2009, 79: 224101−224117.
[29] BAGOT P A J, SILK O B W, DOUGLAS J O, PEDRAZZINI S, CRUDDEN D J, MARTIN T L, HARDY M C, MOODY M P, REED R C. An atom probe tomography study of site preference and partitioning in a nickel-based superalloy [J]. Acta Materialia, 2017, 125: 156−165.
[30] REED R C, YEH A C, TIN S, BABU S S, MILLER M K. Identification of the partitioning characteristics of ruthenium in single crystal superalloys using atom probe tomography [J]. Scripta Materialia, 2004, 51: 327−331.
[31] XU Yu-lai, ZHANG Lei, LI Jun, XIAO Xue-shan, CAO Xiu-li, JIA Guo-qing, SHEN Zhi. Relationship between Ti/Al ratio and stress-rupture properties in nickel-based superalloy [J]. Materials Science and Engineering A, 2012, 544: 48−53.
[32] JIANG Chao, GLEESON B. Site preference of transition metal elements in Ni_3Al [J]. Scripta Materialia, 2006, 55: 433−436.
[33] RICE J R. Dislocation nucleation from a crack tip: An analysis based on the peierls concept [J]. Journal of Mechanics and Physics of Solids, 1992, 40: 239−271.
[34] SUN Yue-min, BELTZ G E. RICE J R. Estimates from atomic models of tension-shear coupling in dislocation nucleation from a crack tip [J]. Materials Science and Engineering A, 1993, 170: 67−85.
[35] RICE J R, BELTZ GLENN E. The activation energy for dislocation nucleation at a crack [J]. Journal of Mechanics and Physics of Solids, 1994, 42: 333−360.
[36] HIDEJI S. Segregation of solute atoms to stacking faults [J]. Journal of the Physical Society Japan, 1962, 17: 322−325.
[37] EURICH N C, BRISTOWE P D. Segregation of alloying elements to intrinsic and extrinsic stacking faults in γ'-Ni_3Al via first principles calculations [J]. Scripta Materialia, 2015, 102: 87−90.
[38] PAIDAR V, POPE D P, VITEK V. A theory of the anomalous yield behavior in $L1_2$ ordered alloys [J]. Acta Materialia, 1984, 32: 435−448.
[39] YI Zhou, PENG Ping. Impact of Re-clustering on resistances to dislocation slip mediated plastic deformations in γ matrix phases [J]. Computational Materials Science, 2020, 172: 109314.
[40] LI Yu-juan, HU Qing-miao, XU Dong-sheng, YANG Rui. Strengthening of γ-TiAl-Nb by short-range ordering of point defects [J]. Intermetallics, 2011, 19: 793−796.
[41] PENG Li, PENG Ping, LIU Yun-guo, HE Shuang, WEI Hua, JIN Tao, HU Zhuang-qi. The correlation between Re and P and their synergetic effect on the rupture strength of the γ-Ni/γ'-Ni_3Al interface [J]. Computational Materials Science, 2012, 63: 292−302.

以 W 取代 Re 对 γ'-Ni_3Al 相位错滑移调制蠕变的影响

易 洲，胥云雷，彭 平，陈江华

湖南大学 材料科学与工程学院，长沙 410082

摘 要： γ'-Ni_3Al 相在高温下的反常流变行为与 1/2⟨110⟩{111}超级部分位错的交滑移密切相关。沿最低能量路径获得的广义堆垛层错能曲线(即 Γ 面)可以提供大量有关位错形核和运动的信息。采用第一性原理计算，研究 Re、W、Mo、Ta、Ti 单掺杂与双掺杂对 γ'-Ni_3Al 相 Γ 面和理想剪切强度 τ_{max} 的影响。与 Re 掺杂的情形类似，W 在堆垛层错处的 Suzuki 偏聚可阻止 1/6⟨112⟩{111} Shockley 部分位错的运动和促进 1/2⟨110⟩{111}超级部分位错的交滑移。当 Re 被 W 部分取代时，$\gamma_{APB}^{111}/\gamma_{APB}^{001}$ 的降低表明 γ'相在高温下的反常流变行为不如双 Re 掺杂，但 τ_{max} 的增加却表明镍基单晶高温合金的蠕变断裂强度在一定程度上可从中受益，尤其是 Re 和 W 在 Al−Al 位的共偏聚。当点缺陷 $X1_{Al}$ 和 $X2_{Al}$ 之间的相互作用采用关联能函数 $\Delta E^{X1_{Al}+X2_{Al}}(d)$ 来表征时，无论是吸引还是排斥，强关联都不利于 γ'相屈服强度的提高。

关键词： 镍基单晶高温合金；γ'-Ni_3Al；广义堆垛层错能；理想剪切强度；位错；交滑移

(Edited by Bing YANG)